Article

Allosterically Regulated Supramolecular Catalysis of Acyl Transfer Reactions for Signal Amplification and Detection of Small Molecules

Martin S. Masar, Nathan C. Gianneschi, Christopher G. Oliveri, Charlotte L. Stern, SonBinh T. Nguyen, and Chad A. Mirkin

J. Am. Chem. Soc., **2007**, 129 (33), 10149-10158• DOI: 10.1021/ja0711516 • Publication Date (Web): 27 July 2007

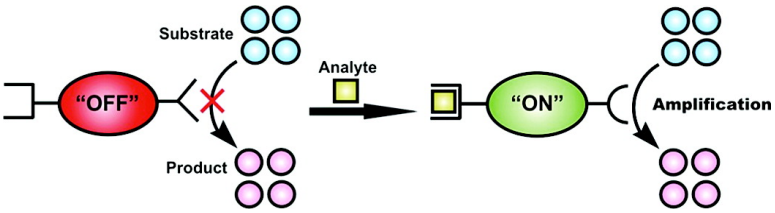

More About This Article

Additional resources and features associated with this article are available within the HTML version:

- Supporting Information
- Links to the 18 articles that cite this article, as of the time of this article download
- Access to high resolution figures
- Links to articles and content related to this article
- Copyright permission to reproduce figures and/or text from this article

View the Full Text HTML

J|A|C|S
ARTICLES
Published on Web 07/27/2007

Allosterically Regulated Supramolecular Catalysis of Acyl Transfer Reactions for Signal Amplification and Detection of Small Molecules

Martin S. Masar III, Nathan C. Gianneschi, Christopher G. Oliveri, Charlotte L. Stern, SonBinh T. Nguyen, and Chad A. Mirkin*

Contribution from the Department of Chemistry and the Institute of Nanotechnology, 2145 Sheridan Road, Evanston, Illinois 60208-3113

Received February 16, 2007; E-mail: chadnano@northwestern.edu

Abstract: The advent of methods for the construction of supramolecular assemblies provides a route to exploring the benefits of artificial allosteric catalysts. To expand our ability to control reactions using supramolecular catalysts capable of changing shape in response to chemical input signals, we report the development and high yield syntheses of multidomain modular supramolecular catalysts. These structures can be chemically interconverted between relatively inactive and catalytically active states depending on their shape. Furthermore, this class of supramolecular catalysts can be made to respond to a range of analytes via the introduction of specific structure control elements responsible for binding analyte molecules. Herein, we describe several of these catalysts and their ability to regulate acyl transfer reactions allosterically. In addition, the generality of this approach to signal amplification and detection is examined by incorporating the acyl transfer reaction into a small molecule detection scheme consisting of (i) analyte binding to structure control sites of the catalytic supramolecular assemblies, (ii) enhanced catalytic activity turned on by the resulting shape change, thereby allowing for signal amplification of the binding event, and (iii) signal detection by analysis of the products of the catalytic reaction.

Introduction

Cooperative interactions are ubiquitous in biological systems. By understanding how to utilize similar interactions in synthetic systems, chemists may be able to harness new and otherwise inaccessible chemistry. Ultimately, when one has the ability to synthesize compounds containing large well-defined cavities,[1−7] species that can arrange molecules and metal ions in a specific and predictable fashion can be designed for catalysis and detection of guest molecules. If these systems are made addressable, such that they respond to chemical or physical input signals, arrays that can perform multiple switchable functions auto-catalytically, cross-catalytically, and with chemical feedback can be developed. These are functions performed routinely by biological systems but are rare in synthetic ones.[8] Chemists have developed several strategies for the assembly of supramolecular architectures that exhibit atypical and often times complex functions.[1−4,9−17] Indeed, the construction of supramolecular assemblies via metal coordination chemistry and hydrogen bonding has provided access to many potentially useful species.[18−36] Of particular interest is the utility of architectures

(1) Holliday, B. J.; Mirkin, C. A. *Angew. Chem., Int. Ed.* **2001**, *40*, 2022−2043.
(2) Leininger, S.; Olenyuk, B.; Stang, P. J. *Chem. Rev.* **2000**, *100*, 853−908.
(3) Caulder, D. L.; Raymond, R. N. *Acc. Chem. Res.* **1999**, *32*, 975−982.
(4) Fujita, M.; Tominaga, M.; Hori, A.; Therrien, B. *Acc. Chem. Res.* **2005**, *38*, 371−380.
(5) Seidel, S. R.; Stang, P. J. *Acc. Chem. Res.* **2002**, *35*, 972−983.
(6) Fujita, M. *Acc. Chem. Res.* **1999**, *32*, 53−61.
(7) Fujita, M.; Umemoto, K.; Yoshizawa, M.; Fujita, N.; Kusukawa, T.; Biradha, K. *Chem. Commun.* **2001**, *6*, 509−518.
(8) Ashkenasy, G.; Jagasia, R.; Yadav, M.; Ghadiri, M. R. *Proc. Natl. Acad. Sci. U.S.A.* **2004**, *101*, 10872−10877.
(9) Conn, M. M.; Rebek, J. *Chem. Rev.* **1997**, *97*, 1647−1668.
(10) Fyfe, M. C. T.; Stoddart, J. F. *Acc. Chem. Res.* **1997**, *30*, 393−401.
(11) Balzani, V.; Credi, A.; M., R. F.; Stoddart, J. F. *Angew. Chem., Int. Ed.* **2000**, *39*, 3348−3391.
(12) Collin, J.-P.; Dietrich-Buchecker, C.; Gavina, P.; Jimenez-Molero, M. C.; Sauvage, J.-P. *Acc. Chem. Res.* **2001**, *34*, 477−487.
(13) Cotton, F. A.; Lin, C.; Murillo, C. A. *Acc. Chem. Res.* **2001**, *34*, 759−771.
(14) Lee, S.-J.; Hu, A.; Lin, W. *J. Am. Chem. Soc.* **2002**, *124*, 12948−12949.
(15) Yoshizawa, M.; Tamura, M.; Fujita, M. *J. Am. Chem. Soc.* **2004**, *126*, 6846−6847.
(16) Ohmori, O.; Kawano, M.; Fujita, M. *J. Am. Chem. Soc.* **2004**, *126*, 16292−16293.
(17) Nakabayashi, K.; Kawano, M.; Yoshizawa, M.; Ohkoshi, S. i.; Fujita, M. *J. Am. Chem. Soc.* **2004**, *126*, 16694−16695.
(18) Kang, J.; Himersson, G.; Santamaria, J.; Rebek, J. *J. Am. Chem. Soc.* **1998**, *120*, 3650−3656.
(19) Ziegler, M.; Brumaghim, J. L.; Raymond, K. N. *Angew. Chem., Int. Ed.* **2000**, *39*, 4119−4121.
(20) Merlau, M. L.; del Pilar Mejia, M.; Nguyen, S. T.; Hupp, J. T. *Angew. Chem., Int. Ed.* **2001**, *40*, 4239−4242.
(21) Lee, S. J.; Lin, W. *J. Am. Chem. Soc.* **2002**, *124*, 4554−4555.
(22) Chen, J.; Korner, S.; Craig, S. L.; Rudkevich, D. M.; Rebek, J., Jr. *Nature* **2002**, *415*, 385−386.
(23) Kusukawa, T.; Nakai, T.; Okano, T.; Fujita, M. *Chem. Lett.* **2003**, *32*, 284−285.
(24) Hua, J.; Lin, W. *Org. Lett.* **2004**, *6*, 861−864.
(25) Gianneschi, N. C.; Tiekink, E. R. T.; Rendina, L. M. *J. Am. Chem. Soc.* **2000**, *122*, 8474−8479.
(26) Ono, K.; Yoshizawa, M.; Kato, T.; Watanabe, K.; Fujita, M. *Angew. Chem., Int. Ed.* **2007**, *46*, 1803−1806.
(27) Yang, H. B.; Hawkridge, A. M.; Huang, S. D.; Das, N.; Bunge, S. D.; Muddiman, D. C.; Stang, P. J. *J. Am. Chem. Soc.* **2007**, *129*, 2120−2129.
(28) Yang, H. B.; Ghosh, K.; Arif, A. M.; Stang, P. J. *J. Org. Chem.* **2006**, *71*, 9464−9469.
(29) Yang, H. B.; Ghosh, K.; Das, N.; Stang, P. J. *Org. Lett.* **2006**, *8*, 3991−3994.
(30) Huang, F.; Yang, H. B.; Das, N.; Maran, U.; Arif, A. M.; Gibson, H. W.; Stang, P. J. *J. Org. Chem.* **2006**, *71*, 6623−6625.

possessing the enzyme-like property of being able to arrange substrates for reaction within a well-defined cavity.[18−24,37−53]

Our group has focused on demonstrating the concept of allosteric regulation in abiotic catalytic systems.[54−57] Allosteric regulation involves the binding of a signaling molecule to a site distinct from the catalytic site. While this regulatory mechanism is found throughout biology, it remains a little explored application in man-made systems.[58] A key feature of this approach is that the allosteric binding event causes a structural change that affects the catalytic activity of the entire supramolecular structure. The inherent chemical orthogonality common to allosteric regulation makes this type of control very useful in the temporal control of enzyme activity in natural systems. The goal of bridging the gap between synthetic and natural allosteric systems has prompted the development of a number of abiotic systems displaying many of the features found in naturally occurring allosterically regulated systems. Specifically, the Weak-Link Approach (WLA) to supramolecular coordination chemistry allows one the ability to build large multimetallic macrocyclic complexes that are capable of being chemically interconverted between "condensed" and "open" states in situ using small molecules (Chart 1).[59] This has allowed us to design a series of allosteric catalysts with reaction centers that affect shape and, concomitantly, catalytic activity.[54−57]

Chart 1. Examples of the Ancillary Ligands Employed Using the Weak-Link Approach

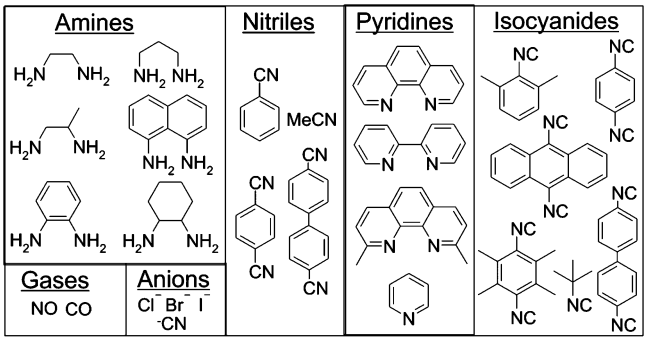

These initial studies have led to the development of a novel catalytic amplification and detection scheme (Scheme 1) based upon supramolecular Rh^I and metal-salen containing complexes prepared via the WLA.[56] This amplification method relies on analyte binding to a supramolecular assembly, which subsequently induces a shape and cavity size change that accelerates a catalytic event generating a detectable molecule. In this way, a small number of binding events can yield a large amount of detectable product, thereby providing a method for signal amplification, a strategy which mimics that used in biological signal transduction. Related synthetic and semi-synthetic signal amplification schemes have attracted recent attention in the context of chemical sensing.[60−62] In these systems, the products of the catalytic amplification reaction can be detected via a variety of methods, including gas chromatography or more convenient fluorophore probe strategies, if the product is fluorescent or if a fluorescent indicator is used. Our initial demonstration of an artificial allosteric catalyst behaving as a molecular sensor, along with studies into the generality of the WLA, has led us to investigate the scope and extent of chemical control over this type of sensor based upon metallosupramolecular allosteric catalysts. Herein, we explore how different small molecules and ions, such as diimines, isocyanides, CO, and Cl^-, can be used as allosteric regulators to control catalytic activity. The significance of these results in the context of chemical sensing through catalytic amplification is also discussed. This system provides a rare example of an abiotic assay for small molecules that has the capability to amplify and detect low analyte quantities in a manner similar to that of enzyme-linked immunosorbent assays (ELISAs) for proteins.[63]

Experimental Section

General Procedures. Unless otherwise noted, all reactions and manipulations were performed under an atmosphere of dry nitrogen using standard Schlenk and glovebox techniques. Tetrahydrofuran (THF), diethyl ether (Et_2O), dichloromethane (CH_2Cl_2), acetonitrile (MeCN), and hexanes were purified by published methods.[64,65] All solvents were degassed with nitrogen prior to use. Deuterated solvents were purchased and used as received from Cambridge Isotopes

(31) Yang, H. B.; Das, N.; Huang, F.; Hawkridge, A. M.; Muddiman, D. C.; Stang, P. J. *J. Am. Chem. Soc.* **2006**, *128*, 10014−10015.
(32) Jude, H.; Disteldorf, H.; Fischer, S.; Wedge, T.; Hawkridge, A. M.; Arif, A. M.; Hawthorne, M. F.; Muddiman, D. C.; Stang, P. J. *J. Am. Chem. Soc.* **2005**, *127*, 12131−12139.
(33) Chatterjee, B.; Noveron, J. C.; Resendiz, M. J. E.; Liu, J.; Yamamoto, T.; Parker, D.; Cinke, M.; Nguyen, C. V.; Arif, A. M.; Stang, P. J. *J. Am. Chem. Soc.* **2004**, *126*, 10645−10656.
(34) Mukherjee, P. S.; Das, N.; Kryschenko, Y. K.; Arif, A. M.; Stang, P. J. *J. Am. Chem. Soc.* **2004**, *126*, 2464−2473.
(35) Kryschenko, Y. K.; Seidel, S. R.; Arif, A. M.; Stang, P. J. *J. Am. Chem. Soc.* **2003**, *125*, 5193−5198.
(36) Dinolfo, P. H.; Hupp, J. T. *Chem. Mater.* **2001**, *13*, 3113−3125.
(37) Cacciapaglia, R.; Di Stefano, S.; Mandolini, L. *Acc. Chem. Res.* **2004**, *37*, 113−122.
(38) Mackay, L. G.; Wylie, R. S.; Sanders, J. K. M. *J. Am. Chem. Soc.* **1994**, *116*, 3141−3142.
(39) Sanders, J. K. M. *Chem.-Eur. J.* **1998**, *4*, 1378−1383.
(40) Kelly, T. R.; Zhao, C.; Bridger, G. J. *J. Am. Chem. Soc.* **1989**, *111*, 3744−3745.
(41) Kelly, T. R.; Bridger, G. J.; Zhao, C. *J. Am. Chem. Soc.* **1990**, *112*, 8024−8034.
(42) Ohsaki, K.; Konishi, K.; Aida, T. *Chem. Commun.* **2002**, 1690−1691.
(43) Chen, J.; Rebek, J. *Org. Lett.* **2002**, *4*, 327−329.
(44) Leung, D. H.; Bergman, R. G.; Raymond, K. N. *J. Am. Chem. Soc.* **2006**, *128*, 9781−9797.
(45) Fiedler, D.; vanHalbeek, H.; Bergman, R. G.; Raymond, K. N. *J. Am. Chem. Soc.* **2006**, *128*, 10240−10252.
(46) Fiedler, D.; Bergman, R. G.; Raymond, K. N. *Angew. Chem., Int. Ed.* **2006**, *45*, 745−748.
(47) Fiedler, D.; Leung, D. H.; Bergman, R. G.; Raymond, K. N. *Acc. Chem. Res.* **2005**, *38*, 349−358.
(48) Leung, D. H.; Fiedler, D.; Bergman, R. G.; Raymond, K. N. *Angew. Chem., Int. Ed.* **2004**, *43*, 963−966.
(49) Fiedler, D.; Pagliero, D.; Brumaghim, J. L.; Bergman, R. G.; Raymond, K. N. *Inorg. Chem.* **2004**, *43*, 846−848.
(50) Fiedler, D.; Leung, D. H.; Bergman, R. G.; Raymond, K. N. *J. Am. Chem. Soc.* **2004**, *126*, 3674−3675.
(51) Fiedler, D.; Bergman, R. G.; Raymond, K. N. *Angew. Chem., Int. Ed.* **2004**, *43*, 6748−6751.
(52) Pluth, M. D.; Bergman, R. G.; Raymond, K. N. *Science* **2007**, *316*, 85−88.
(53) Yoshizawa, M.; Tamura, M.; Fujita, M. *Science* **2006**, *312*, 251−254.
(54) Gianneschi, N. C.; Bertin, P. A.; Nguyen, S. T.; Mirkin, C. A.; Zakharov, L. N.; Rheingold, A. L. *J. Am. Chem. Soc.* **2003**, *125*, 10508−10509.
(55) Gianneschi, N. C.; Cho, S.-H.; Nguyen, S. T.; Mirkin, C. A. *Angew. Chem., Int. Ed.* **2004**, *43*, 5503−5507.
(56) Gianneschi, N. C.; Nguyen, S. T.; Mirkin, C. A. *J. Am. Chem. Soc.* **2005**, *127*, 1644−1645.
(57) Oliveri, C. G.; Gianneschi, N. C.; Nguyen, S. T.; Mirkin, C. A.; Stern, C. L.; Wawrzak, Z.; Pink, M. *J. Am. Chem. Soc.* **2006**, *128*, 16286−16296.
(58) Kovbasyuk, L.; Kramer, R. *Chem. Rev.* **2004**, *104*, 3161−3187.
(59) Gianneschi, N. C.; Masar, M. S., III; Mirkin, C. A. *Acc. Chem. Res.* **2005**, *38*, 825−837.
(60) Saghatelian, A.; Guckian, K. M.; Thayer, D. A.; Ghadiri, M. R. *J. Am. Chem. Soc.* **2003**, *125*, 344−345.
(61) Zhu, L.; Anslyn, E. V. *Angew. Chem., Int. Ed.* **2006**, *45*, 1190−1196.
(62) Anslyn, E. V. *J. Org. Chem.* **2007**, *72*, 687−699.
(63) Walsh, J. H.; Yalow, R.; Berson, S. A. *J. Infect. Dis.* **1970**, *121*, 550.
(64) Armarego, W. L. F.; Perrin, D. D. *Purification of Laboratory Chemicals*; Butterworth-Heinemann: Oxford, 1996.
(65) Pangborn, A. B.; Giardello, M. A.; Grubbs, R. H.; Rosen, R. K.; Timmers, F. J. *Organometallics* **1996**, *15*, 1518−20.

Scheme 1. Supramolecular Allosteric Catalytic Signal Amplifier[a]

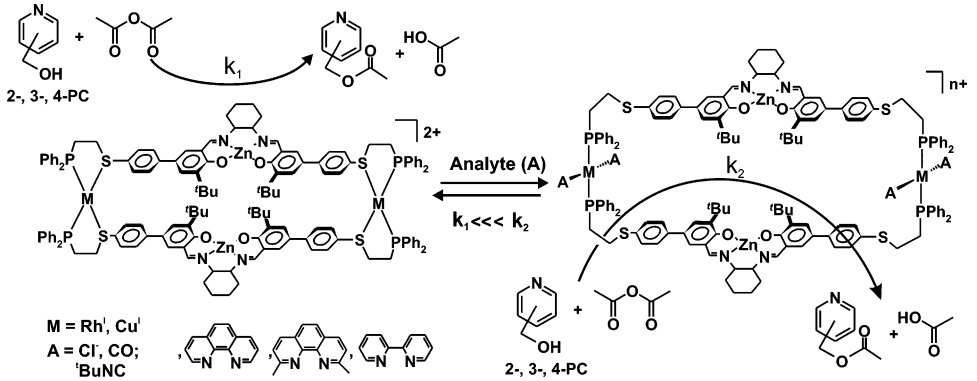

[a] A slow background reaction occurs in the absence of analyte (A). Analyte binding opens the cavity and allows substrate molecules (pyridylcarbinol and acetic anhydride) to enter where they undergo a fast intramolecular reaction generating acetic acid and acetoxymethylpyridine.

Scheme 2. Synthesis of Allosteric Supramolecular Assemblies[a]

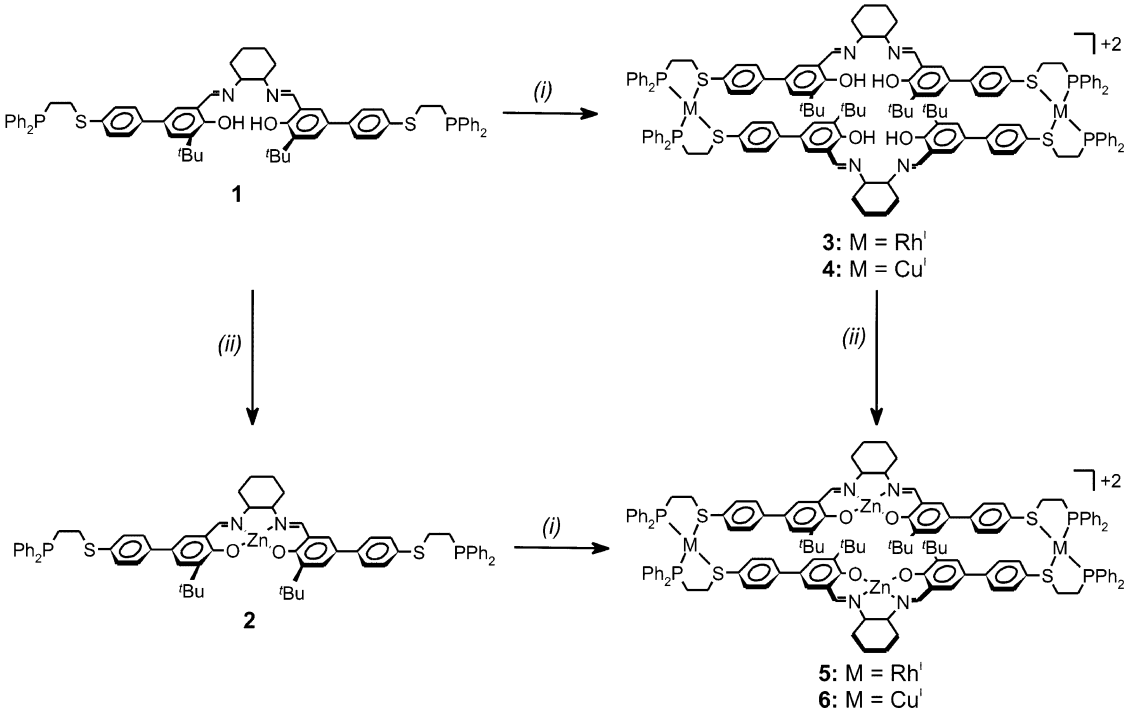

[a] All reactions were performed at 25 °C. Counterions are PF_6^- (**4**, **6**) or BF_4^- (**3**, **5**). All cyclohexyl salen backbones have (*R*,*R*) stereochemistry. Reagents and solvents: (i) for **3**, **5**, $[Rh(NBD)_2]BF_4$, CH_2Cl_2; for **4**, **6**, $[Cu(MeCN)_4]PF_6$, CH_2Cl_2. (ii) Et_2Zn (1.0 M in hexanes), THF.

Laboratories. Ligand **1** and complexes **2, 3**, **5**, **7**,[54] and **9**[66] were prepared as previously reported (Scheme 2). All other chemicals were obtained from commercial sources and used as received unless otherwise noted.

Physical Measurements. $^{31}P\{^1H\}$ NMR spectra were recorded on a Varian 300 MHz Gemini FT-NMR spectrometer at 121.53 MHz and referenced relative to an external 85% H_3PO_4 standard. ^1H NMR spectra were obtained using a Varian Gemini 300 MHz FT-NMR spectrometer and referenced relative to tetramethylsilane. All chemical shifts are reported in ppm. FT-IR spectra were obtained using a ThermoNicolet Nexus 670 FT-IR and a solution cell with NaCl windows. Electrospray mass spectra (ESIMS) were obtained on a Micromas Quatro II triple quadrapole mass spectrometer. Gas chromatography (GC) analyses of reaction mixtures were carried out on a computer-interfaced Agilent Technologies 6890 Network instrument equipped with a flame ionization detector (FID). The column used during the course of this work was a 30-m HP-5 capillary column with a 0.32-mm inner diameter and a 0.25-μm film thickness. GC yields were determined through integration of the product peak against biphenyl (internal standard) using pre-established response factors. GC retention times of products were confirmed with analytically pure samples. Elemental analyses were obtained from Quantitative Technologies Inc., Whitehouse, NJ.

Synthesis of the Free-Base Salen Macrocycle $[(1)_2Rh_2](BF_4)_2$ (3). A small vial was charged with $[Rh(NBD)Cl]_2$ (0.063 g, 0.14 mmol), $AgBF_4$ (0.054 g, 0.28 mmol), and CH_2Cl_2 (2 mL). This solution was stirred for 2 h, filtered dropwise through Celite into a Schlenk flask, and diluted with CH_2Cl_2 (150 mL) to give an orange solution. Compound **1** (0.30 g, 0.27 mmol) in CH_2Cl_2 (150 mL) was added to the "Rh" solution via a dropping funnel over 1 h at −78 °C. The solution was allowed to slowly warm to room temperature and stir for 48 h. The solvent was removed in vacuo to yield a yellow microcrystalline solid, which was dissolved in a minimal amount of CH_2Cl_2 and filtered through Celite. Following solvent removal, the yellow solid

(66) Dixon, F. M.; Eisenberg, A. E.; Farrell, J. R.; Mirkin, C. A.; Liable-Sands, L. M.; Rheingold, A. L. *Inorg. Chem.* **2000**, *39*, 3432−3433.

was recrystallized from CH_2Cl_2/pentane to yield compound **3** (300 mg, 92%). ^{1}H NMR (CD_2Cl_2): δ 1.37 (s, 36H, C(C*H*$_3$)$_3$), 1.68−2.20 (br m, 16H, cyclohexyl), 2.23−2.66 (m, 16H, C*H*$_2$P and C*H*$_2$S), 3.53 (m, 4H, cyclohexyl), 7.08−7.51 (m, 64H, aromatic), 8.05 (s, 4H, N=C*H*), 14.4 (s, 4H, O*H*). ^{31}P{^{1}H} NMR (CD_2Cl_2): δ 64.9 (d, J_{Rh-P} = 162 Hz). ESIMS (*m/z*): $[C_{136}H_{144}O_4N_4S_4P_4Rh_2]^{2+}$: calcd. = 1178.3; expt. = 1178.3. Anal. Calcd for $[C_{136}H_{144}O_4N_4S_4P_4Rh_2B_2F_8]\cdot CH_2Cl_2$: C, 62.92; H, 5.63; N, 2.14. Found: C, 63.20; H, 5.54; N, 1.93.

Synthesis of the Free-Base Salen Macrocycle [(1)$_2$Cu$_2$](PF$_6$)$_2$ (4). In a Schlenk flask, ligand **1** (100.0 mg, 0.0930 mmol) was dissolved in CH_2Cl_2 (8 mL). A solution of Cu(MeCN)$_4$PF$_6$ (35.0 mg, 0.0940 mmol) in CH_2Cl_2 (5 mL) and MeCN (3 mL) was added to the stirring ligand solution to give a pale yellow solution. After the mixture was stirred for 2 h, solvent was removed and the resulting yellow solid was dried under vacuum. Recrystallization from CH_2Cl_2/Et_2O afforded **4** as a yellow microcrystalline powder (103 mg, 86%). ^{1}H NMR (CD_2Cl_2): δ 1.35 (s, 36H, C(C*H*$_3$)$_3$), 1.80−2.04 (br m, 16H, cyclohexyl), 2.67 (m, 8H, C*H*$_2$P), 3.23 (m, 8H, C*H*$_2$S), 3.39 (s, 4H, cyclohexyl), 7.3−7.7 (br m, 64H, aromatic), 8.30 (s, 4H, N=C*H*), 14.2 (s, 4H, O*H*). ^{31}P{^{1}H} NMR (CD_2Cl_2): δ 0.3 (s), −143.3 (sept, PF_6). ESIMS (*m/z*) $[C_{136}H_{144}O_4N_4S_4P_4Cu_2]^{2+}$: calcd. = 1138.9; expt. = 1138.8. Anal. Calcd for $C_{136}H_{144}O_4N_4S_4P_4Cu_2P_2F_{12}$: C, 63.61; H, 5.65; N, 2.18. Found: C, 63.33; H, 5.54; N, 2.54.

Synthesis of the Closed Zn^{II}-Salen Macrocycle [(1)$_2$Cu$_2$Zn$_2$](PF$_6$)$_2$ (6). Method A. In a Schlenk flask, **2** (155 mg, 0.136 mmol) was dissolved in CH_2Cl_2 (5 mL). A solution of Cu(MeCN)$_4$PF$_6$ (44 mg, 0.136 mmol) in CH_2Cl_2 (5 mL) was added to the stirring ligand solution to give a yellow solution. After the mixture was stirred for 2 h, solvent was removed in vacuo. Recrystallization from CH_2Cl_2/Et_2O afforded **6** as a yellow microcrystalline solid.

Method B. In a Schlenk flask, complex **4** (60 mg, 23.4 μmol) was dissolved in THF (15 mL). A solution of Et_2Zn in hexanes (60 μL, 1.0 M, 60 μmol) was added to the stirring solution to give a yellow solution. After the mixture was stirred for 2 h, solvent was removed in vacuo to yield a yellow solid. Recrystallization from CH_2Cl_2/Et_2O afforded **6** as a yellow microcrystalline solid (156 mg, 85%). ^{1}H NMR (CD_2Cl_2): δ 1.32 (s, 36H, C(C*H*$_3$)$_3$), 2.1−2.3 (m, 16H, cyclohexyl), 2.63 (m, 8H, C*H*$_2$P), 3.20 (br m, 12H, C*H*$_2$S and cyclohexyl), 6.8−7.6 (br m, 64H, aromatic), 8.63 (s, 4H, N=C*H*). ^{31}P{^{1}H} NMR (CD_2Cl_2): δ 1.1 (s), −143.2 (sept, PF_6). ESIMS (*m/z*) $[C_{136}H_{140}O_4N_4S_4P_4Cu_2Zn_2]^{2+}$: calcd. = 1202.3; expt. = 1202.4. Anal. Calcd for $C_{136}H_{140}O_4N_4S_4P_4Cu_2Zn_2P_2F_{12}$: C, 63.66; H, 5.58; N, 2.18. Found: C, 63.62; H, 5.72; N, 2.33.

Synthesis of the Open Zn^{II}-Salen Macrocycle [(1)$_2$Cu$_2$Zn$_2$phen$_2$](PF$_6$)$_2$ (8). In an air-free NMR tube, complex **6** (15 mg, 5.6 μmol) in CD_2Cl_2 (0.4 mL) was treated with a solution of 1,10-phenanthroline (phen) (2 mg, 11 μmol) in CD_2Cl_2 (0.4 mL) to yield a red-orange solution, which contained analytically pure **8** as determined by ^{31}P-{^{1}H} and ^{1}H NMR spectroscopy. ^{1}H NMR (CD_2Cl_2): δ 1.2−1.6 (s, 36H, C(C*H*$_3$)$_3$), 1.8−2.3 (br m, 16H, cyclohexyl), 2.65 (m, 8H, C*H*$_2$P), 3.08 (br m, 12H, C*H*$_2$S and cyclohexyl), 6.8−7.6 (br m, 64H, aromatic), 7.83 (m, 4H, phen), 8.05 (s, 4H, phen), 8.38 (m, 4H, phen), 8.60 (s, 4H, N=C*H*), 8.77 (m, 4H, phen). ^{31}P{^{1}H} NMR (CD_2Cl_2): δ −4.4 (s), −143.3 (sept, PF_6). ESIMS (*m/z*) $[C_{136}H_{140}O_4N_4S_4P_4Cu_2Zn_2C_{24}H_{16}N_4]^{2+}$: calcd. = 1382.5; expt. = 1382.4.

General Procedure for Catalysis Experiments. The formation of 2-, 3-, and 4-acetoxymethylpyridine was monitored by gas chromatography (GC-FID) relative to an internal standard (biphenyl). All reactions were performed at room temperature in CH_2Cl_2 under N_2 unless stated otherwise.

Example Procedure for Experiments Using Rh^I-Based Catalysts. Complex **5** (0.5 mM), biphenyl (1.5 mM), 3-pyridylcarbinol (1.0 mM), and acetic anhydride (1.0 mM) in CH_2Cl_2 were added to a 10 mL Schlenk flask. In a second Schlenk flask, these reagents and benzyltriethylammonium chloride (1.0 mM) were added followed by introduction of CO (1 atm). The total volume of these reactions was 2.0 mL. At various points (typically 0.5 h apart), an aliquot (0.1 mL) was taken from the solution and added to Et_2O (2.0 mL). These solutions were passed through a plug of Celite (3 cm × 0.5 cm). The resulting samples were used for GC analysis. Genuine samples of the catalytic products were used to confirm that this sample processing procedure does not alter their concentrations with respect to the internal standard (biphenyl).

Example Procedure for Experiments Using Cu^I-Based Catalysts. Complex **6** (0.5 mM), biphenyl (1.5 mM), 4-pyridylcarbinol (1.0 mM), and acetic anhydride (1.0 mM) in CH_2Cl_2 were added to a 10 mL Schlenk flask. In a second Schlenk flask, these reagents and 1,10-phenanthroline (1.0 mM) were added. The total volume of these reactions was 2.0 mL. At various points (typically 0.5 h apart), an aliquot (0.1 mL) was taken from the solution and added to pentane (0.5 mL). This solution was loaded onto a plug of Celite (3 cm × 0.5 cm), followed by elution of substrates and products (but not catalyst) with Et_2O (2 mL). The resulting samples were used for GC analysis.

For catalyst loading experiments conducted with **5** and **6**, the concentrations of all reagents were kept constant except for the catalyst (e.g., Figure 11). In the studies of the different allosteric effectors, the conditions were identical to those described above, with the exception of which compound was added to the second flask (i.e., 2,2′-bipyridine, neocuproine, etc.) (e.g., Figure 13).

Control Experiments. Control experiments for the Rh^I-based catalysts were performed as shown in Figure 4. Conditions were as above except for the catalytic species in each of the controls: complex **5** (0.5 mM, 50%), noncatalytic Rh^I macrocycle **9** (0.5 mM, 50%), or Zn^{II} monomer **2** (1 mM, 100%). Similar experiments were conducted with a noncatalytic Cu^I-thioether based macrocycle[67] analogous to **9**. The background reactions for the four different alcoholic substrates (2-, 3-, and 4-pyridylcarbinol and benzyl alcohol) were monitored by GC using the experimental setup described above with the exception that no catalyst was added. Further control experiments with the 2-pyridylcarbinol substrate are shown in Figure 6. In these experiments, the reaction conditions were as described above except when Zn^{II} monomer **2** was used where its concentration was 1 mM.

Fluorometery Experiments. Complex **5** (0.1 mM), 4-pyridylcarbinol (0.1 mM), acetic anhydride (0.1 mM), diethylaminomethylanthracene (1.0 mM), and appropriate amounts of benzyltriethylammonium chloride were added to a series of 10 mL Schlenk flasks, followed by introduction of CO (1 atm). The total volume of the reactions was 2.5 mL of CH_2Cl_2. Aliquots of these solutions (1.5 mL) were placed in fluorescence cells with stir bars. Fluorescence measurements (λ_{ex} = 368 nm, λ_{em} = 415 nm) were taken every 3 min over 12 h while stirring. Identical reactions were run in parallel for these solutions and were photographed under a handheld laboratory UV lamp (Figure 8).

Results and Discussion

The WLA to supramolecular chemistry has been the basis for the synthesis of a novel class of allosteric catalysts.[59] Importantly, a range of metal-coordination environments and ligand combinations have been employed in the WLA providing significant synthetic flexibility for the design of molecules for a specific function.[1,59,66−77] Molecules containing a variety of

(67) Masar, M. S., III; Mirkin, C. A.; Stern, C. L.; Zakharov, L. N.; Rheingold, A. L. *Inorg. Chem.* **2004**, *43*, 4693−4701.
(68) Farrell, J. R.; Mirkin, C. A.; Guzei, I. A.; Liable-Sands, L. M.; Rheingold, A. L. *Angew. Chem., Int. Ed.* **1998**, *37*, 465−467.
(69) Farrell, J. R.; Mirkin, C. A.; Liable-Sands, L. M.; Rheingold, A. L. *J. Am. Chem. Soc.* **1998**, *120*, 11834−11835.
(70) Farrell, J. R.; Eisenberg, A. H.; Mirkin, C. A.; Guzei, I. A.; Liable-Sands, L. M.; Incarvito, C. D.; Rheingold, A. L.; L., S. C. *Organometallics* **1999**, *18*, 4858−4868.
(71) Holliday, B. J.; Farrell, J. R.; Mirkin, C. A.; Lam, K.-C.; Rheingold, A. L. *J. Am. Chem. Soc.* **1999**, *121*, 6316−6317.

metal-binding functional groups have been shown to bind to supramolecular assemblies synthesized via the WLA to generate significant changes in the size and shape of the macrocyclic cavities. These metal-binding functionalities include halide ions,[66] CO,[66,68] nitrogen heterocycles,[67,77] nitriles,[68,70] cyanide,[72] and amines[77] (Chart 1). Importantly, these molecules and ions often react selectively, giving different responses depending on the specific metal and hemilabile ligand combination used to form the primary structure.[59]

To amplify a detection event using an allosteric catalyst, a suitable reaction is needed in which substrates react at significantly different rates in the presence of two or more states of a catalyst.[61] Therefore, through choice of ligand and metal combinations, systems can be developed in which the "on" and "off" states of a catalyst are accessed by the respective presence and absence of analyte. In such a system, it is critical that the chemistry occurring at the catalytic site be orthogonal, or at least not inhibitory, to the chemistry occurring at the regulatory site and vice versa. The ability to change our system in a modular fashion, facilitated by the WLA synthetic methodology, allows for the adjustment of the chemistry at either the structural or the catalytic sites to facilitate the detection of the desired analyte.[57,59]

Our detection scheme consists of three parts: (1) the analyte binding event which takes place at the structure control site within the allosteric catalyst; (2) the catalytic event which occurs at a distal catalytic site and is activated allosterically by analyte binding; and (3) the signaling event in which a product of the catalytic reaction is directly or indirectly detected using a convenient strategy (Scheme 1). To successfully assemble systems that incorporate these functionalities, a suitable amplification reaction needed to be developed and optimized in which allosteric control via interaction of small molecule protagonists with the supramolecular catalysts was demonstrable. Furthermore, a convenient read-out method is required to develop a detection strategy.

In 1994, Sanders and co-workers reported the intramolecular activation of an acyl transfer reaction using a porphyrin-based cage assembled using synthetic organic chemistry.[38] In this case, the reagents (4-pyridylcarbinol and 1-acetylimidazole) are brought into proximity within the porphyrin cage via binding through nitrogen donors to Zn^{II} metal centers bound to the porphyrin ligands. Approximately 10-fold rate increases are observed for the reaction catalyzed by the supramolecular catalyst versus the monomeric catalyst. Thus, the acyl transfer reaction, with suitable reagents, has been shown to be sensitive to effective molarity changes induced by well-defined supramolecular cavities. In addition, related acyl transfer reactions utilizing acetic anhydride in place of acetylimidazole yield acetic acid, suggesting that one could use a readily available pH sensitive dye[78] to monitor the reaction and the amplified sensor response. Consequently, the viability of the acyl transfer reaction as an amplification method for detection using allosteric catalysts synthesized via the WLA has become a primary focus in our studies. One can appreciate the potential for generalization to other bimetallic reactions.

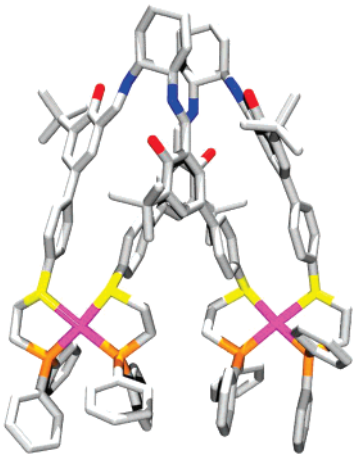

Figure 1. Representation of the X-ray crystal structure of **3**. Hydrogen atoms and counterions have been omitted for clarity. C = gray, Rh = pink, S = yellow, P = orange, N = blue and O = red. The Rh−Rh distance is approximately 6 Å.

Synthesis and Reactivity of Rh^{I} and Cu^{I} Allosteric Catalysts. To study this novel signal transduction method, catalysts **5** and **6** were synthesized via the WLA. The salen moiety of ligand **1** was metalated upon addition of Et_2Zn in THF to give **2**, followed by addition of a Rh^{I} or Cu^{I} source in CH_2Cl_2 (Scheme 2).[54] Compound **5** was previously characterized in the solid-state by a single-crystal X-ray diffraction study.[54] An alternative route for the synthesis of complexes **5** and **6** was investigated by first isolating **3** and **4** in nearly quantitative yield followed by reaction with Et_2Zn. Interestingly, **3** and **4** are 58-membered macrocycles, making them among the largest synthesized via the WLA. These complexes are quite flexible as evidenced by the saddle-like shape adopted by **3** in its X-ray crystal structure (Figure 1). Critically, the specific reactivity of each metal with each of the multiple ligand domains provides a kind of orthogonality that allows for flexibility in the synthesis of the catalysts. Essentially, careful choice of metal starting material provides two potential routes to the same species with the final compound consisting of two structural domains containing Rh^{I} or Cu^{I} metal centers and a catalytic domain containing two Zn^{II} metal centers.[79]

Importantly, the metal−thioether bonds of compounds **5** and **6** are cleaved by small molecules to form flexible macrocycles (**7** and **8**), that have a greater distance between the catalytic Zn^{II}-sites than in **5** or **6** (Scheme 3). To induce this conversion, the Rh^{I}-containing **5** is treated with CO gas (1 atm) in the presence of Cl^- ions (benzyltriethylammonium chloride or bis(triphenylphosphoranylidene)ammonium chloride) in CH_2Cl_2. Significantly, both CO and Cl^- are required to break the thioether/Rh^{I} bonds,[66] leaving the phosphine/Rh^{I} bonds intact. In contrast, the Cu^{I}-containing **6** can be opened with a different set of ancillary ligands, such as 1,10-phenanthroline, and does not require a second ligand to effect the shape change.[67] The significant shape change (rigid/"closed" to flexible/"open") that

(72) Eisenberg, A. H.; Dixon, F. M.; Mirkin, C. A.; Stern, C. L.; Incarvito, C. D.; Rheingold, A. L. *Organometallics* **2001**, *20*, 2052−2058.
(73) Eisenberg, A. H.; Ovchinnikov, M. V.; Mirkin, C. A. *J. Am. Chem. Soc.* **2003**, *125*, 2836−2837.
(74) Masar, M. S., III; Ovchinnikov, M. V.; Mirkin, C. A.; Zakharov, L. N.; Rheingold, A. L. *Inorg. Chem.* **2003**, *42*, 6851−6858.
(75) Brown, A. M.; Ovchinnikov, M. V.; Stern, C. L.; Mirkin, C. A. *J. Am. Chem. Soc.* **2004**, *126*, 14316−14317.
(76) Ovchinnikov, M. V.; Brown, A. M.; Liu, X.; Mirkin, C. A.; Zakharov, L. N.; Rheingold, A. L. *Inorg. Chem.* **2004**, *43*, 8233−8235.
(77) Khoshbin, M. S.; Ovchinnikov, M. V.; Mirkin, C. A.; Zakharov, L. N.; Rheingold, A. L. *Inorg. Chem.* **2005**, *44*, 496−501.
(78) Copeland, G. T.; Miller, S. J. *J. Am. Chem. Soc.* **1999**, *121*, 4306−4307.
(79) Gianneschi, N. C.; Mirkin, C. A.; Zakharov, L. N.; Rheingold, A. L. *Inorg. Chem.* **2002**, *41*, 5326−5328.

Scheme 3 [a]

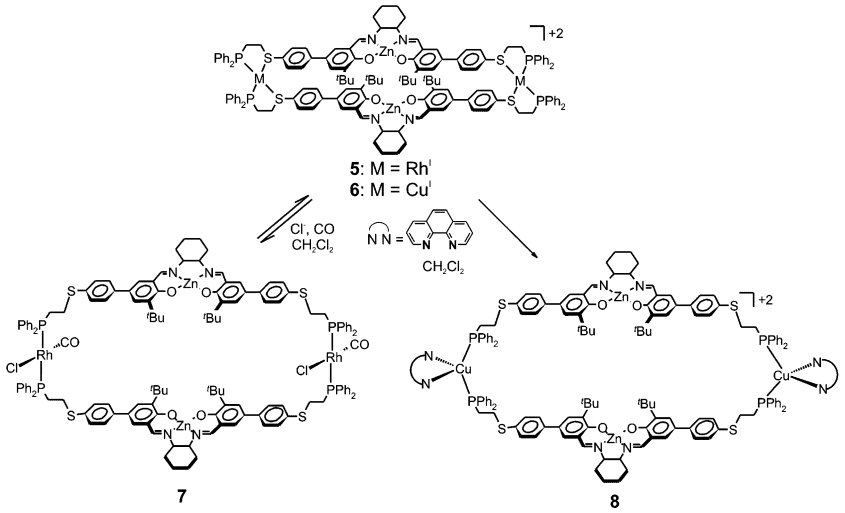

[a] All reactions were performed at 25 °C. Counterions are PF_6^- (**6**, **8**) or BF_4^- (**5**). All cyclohexyl salen backbones have (*R*,*R*) stereochemistry.

occurs upon binding of ancillary ligands was initially used to modulate the rates of the acyl transfer reaction between 1-acetylimidazole and 4-pyridylcarbinol using the supramolecular catalysts **5** and **7**.

Demonstration and Optimization of Allosteric Control over an Acyl Transfer Reaction. An initial examination of the reaction between 4-pyridylcarbinol and 1-acetylimidazole was performed. The hypothesis behind this detection method is that a supramolecular framework incorporating Zn^{II} salen-based ligands would provide a switch between an intermolecular reaction and a predominantly intramolecular reaction.[38] The reactions catalyzed by **5** and **7** are compared to each other and to the uncatalyzed reaction by monitoring the formation of 4-acetoxymethylpyridine by GC-FID (Figure 2). Compound **5** accelerates the reaction via Lewis acid activation of the acetylimidazole (approximately 10-fold rate enhancement), also observed for the same reaction catalyzed by Zn^{II} porphyrin monomers.[38] Importantly, the reaction rate is doubled upon opening **5** with the allosteric activators Cl^- and CO to generate **7** at a catalyst concentration of 0.038 mM. At a higher concentration (0.38 mM), the rate of reaction using **7** as the catalyst is approximately tripled compared to that with **5**. This 2−3-fold rate increase upon opening of the catalyst at these concentrations provided initial evidence that this supramolecular catalyst framework can be used to allosterically control the acyl transfer reaction. Furthermore, control reactions in the absence of catalyst show that the allosteric activators, Cl^- and CO, are not directly involved in the catalytic reaction and are, therefore, suitable analytes for detection (Figure 2).

The allosteric control exhibited by this supramolecular system in the reaction between 1-acetylimidazole and 4-pyridylcarbinol provides a further example of the utility of this type of molecular complex in catalytic regulation.[54,55] To understand and optimize the potential of this catalytic system, further studies into the role of the substrates were undertaken. Hence, the acyl transfer reaction between 4-pyridylcarbinol and acetic anhydride was employed as the signal amplification reaction. We hypothesized this design would provide a switch between a Lewis-acid-catalyzed monometallic reaction and a bimetallic reaction in which the acetic anhydride is activated by one Zn^{II}-salen moiety while in proximity to a pyridylcarbinol molecule bound to another Zn^{II}-center within the supramolecular cavity. Therefore, the bimetallic catalytic pathway provided by the macrocyclic host cavity takes advantage of proximity effects and Lewis-acid activation.[38] Interestingly, the initial reaction rate is increased 20-fold upon opening of **5** with Cl^- and CO to generate **7** at a catalyst concentration of 0.38 mM (Figure 3). In the context of chemical sensing, this rate increase upon opening of the catalyst at these concentrations will provide

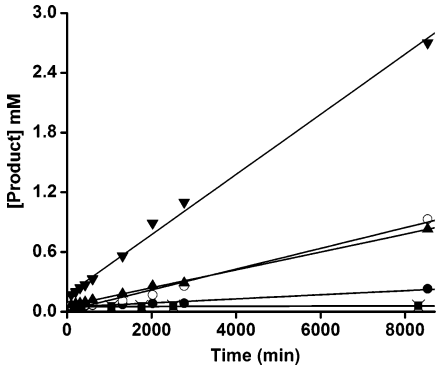

Figure 2. Allosteric control of an acyl transfer reaction. Conditions: 1-acetylimidazole (9.0 mM), 4-pyridylcarbinol (9.0 mM), biphenyl (2.5 mM, internal standard), catalyst, CH_2Cl_2, room temperature. ×, no catalyst; ■, no catalyst + Cl^-/CO; ▲, **5** (0.38 mM); ▼, **7** (0.38 mM); ●, **5** (0.038 mM); ○, **7** (0.038 mM).

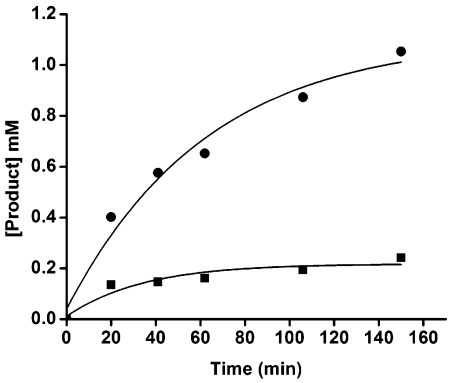

Figure 3. Allosteric control of an acyl transfer reaction. Conditions: acetic anhydride (9.0 mM), 4-pyridylcarbinol (9.0 mM), biphenyl (2.5 mM, internal standard), catalyst (0.38 mM), CH_2Cl_2, room temperature. ■, **5**; ●, **7**.

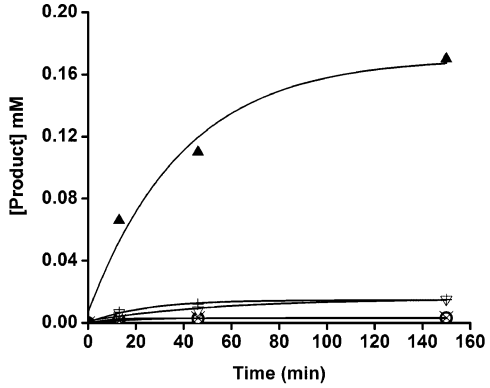

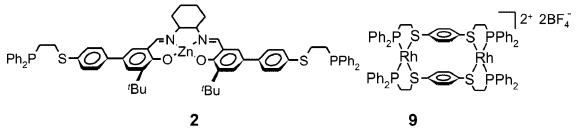

Figure 4. Product (4-acetoxymethylpyridine) concentration versus time for a series of control reactions. Reactions were monitored by GC-FID. Conditions: CH_2Cl_2, room temperature, 4-pyridylcarbinol (1.0 mM), acetic anhydride (1.0 mM), biphenyl (1.5 mM, standard), catalyst, CO (1 atm), and benzyltriethylammonium chloride (2 equiv with respect to catalyst). ▽, **5** (0.5 mM); ▲, **7** (0.5 mM); +, **2** (1.0 mM); ×, **9** (0.5 mM); ○, **9** (0.5 mM) + Cl^-/CO. The cyclohexyl salen backbone has (*R*,*R*) stereochemistry.

greater signal amplification compared to the system that uses 1-acetylimidazole as the acylating agent. In addition, by modifying the acyl transfer reaction to generate acetic acid, one can couple the allosteric amplification to an acid-sensitive fluorescent probe.[56,78]

It is clear that both **5** and **7** catalyze acyl transfer reactions. However, critical to the detection scheme, the catalysis must occur at very different rates. We hypothesize that this rate difference is due to the open cavity of **7** providing access to a predominantly intramolecular reaction pathway. This hypothesis has been supported by a number of control reactions. For instance, complex **5** catalyzes the acyl transfer reaction no more efficiently than the monomeric Zn^{II} salen **2** (Figure 4). Furthermore, the bimetallic Rh^{I}-containing complex **9** does not catalyze the reaction in either closed or open form, suggesting that neither the Rh^{I} metal center nor the benzyltriethylammonium salt are directly involved in the acyl transfer reaction under these conditions. The use of alternative sources of Cl^-, such as PPNCl (bis(triphenylphosphoranylidene)ammonium chloride), gave similar results, further confirming the orthogonality of the chemistry employed to address the hemilabile metal hinge. Additionally, the rate of reaction using benzyl alcohol (BA) in lieu of pyridyl carbinol (PC) does not show a significant dependence on the catalyst used (**5** or **7**) (Figure 5). These data support the hypothesis that the enhanced catalytic effect of **7** is due, at least in part, to the pyridylcarbinol binding to the Zn^{II} centers in a fashion that places the alcohol moiety near an activated acetic anhydride molecule. In addition, it should be noted that the reactions appear to be product inhibited. We hypothesize that this is because a Zn^{II} metal center coordinated to a strongly bound N-donor will be incapable of facilitating Lewis acid activation of acylating reagents. This effect is highlighted in the cases where a weakly coordinating reagent, such as acetic anhydride, is used as the acylating reagent. In these instances, the catalytic reaction must compete for available Zn^{II} metal centers with both product and starting material.

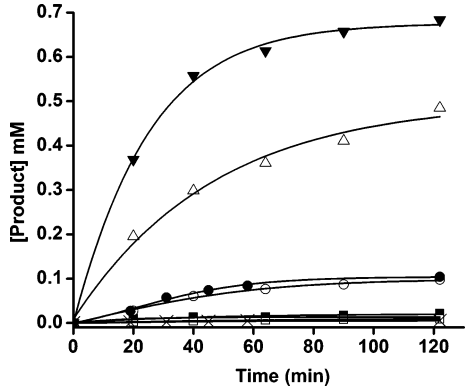

Figure 5. Product (acylated alcohol) concentration versus time for the acyl transfer to the three isomers of pyridylcarbinol (2-, 3- or 4-PC) and benzyl alcohol (BA). Reactions were monitored by GC-FID. Conditions: CH_2Cl_2, room temperature, alcohol (1.0 mM), acetic anhydride (1.0 mM), biphenyl (1.5 mM, standard), catalyst (0.5 mM). ▼, 2PC, **7**; △, 2PC, **5**; ○, 3PC, **7**; □, 3PC, **5**; ●, 4PC, **7**; ×, 4PC, **5**; ■, BA, **7**; +, BA, **5**.

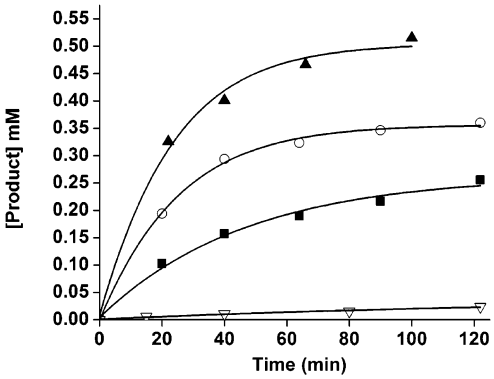

Figure 6. Product (2-acetoxymethylpyridine) concentration versus time for the acyl transfer to 2-pyridylcarbinol with different catalysts. Reactions were monitored by GC-FID. Conditions: CH_2Cl_2, room temperature, 2-pyridylcarbinol (1.0 mM), acetic anhydride (1.0 mM), biphenyl (1.5 mM, standard), and catalyst. ▲, **2** (1.0 mM); ○, **7** (0.5 mM); ■, **5** (0.5 mM); ▽, no catalyst.

In addition to the acylating agent, the role of the alcohol-containing reactant was examined. In these experiments, the three isomers of pyridylcarbinol (2-, 3-, and 4-PC) were studied to determine if any substrate selectivity occurs. As seen in Figure 5, 3- and 4-pyridylcarbinol exhibit increased reaction rates when using catalyst **7** compared to that observed with catalyst **5**, and the rate increases are of similar magnitude for each isomer. Specifically, the ratio of intial rates for open versus closed catalysts for the *para*-isomer is 24, while that using the *meta*-isomer is 18. Interestingly, the reaction rate when 2-pyridyl carbinol is used as the substrate is dramatically increased using either catalyst (Figure 6). For example, the rate of acyl transfer for the *ortho*-isomer is 80−100 times as fast as the *meta*- or *para*-isomers using the closed catalyst **5**. However, the ratio of the initial rates for the open versus the closed catalyst for the *ortho*-isomer is only 2. This behavior is partially explained by comparison of the reaction rates of the uncatalyzed reactions of each of these isomers with acetic anhydride, in which the rate for 2-pyridylcarbinol is approximately 10 times faster than the other isomers. Also, the monomeric Zn^{II} catalyst **2** catalyzes this transformation much faster than the dimeric catalyst (Figure 6). A possible explanation for these results is that 2-pyridylcarbinol is not activated by the Zn^{II} centers. In fact, the proximity of the nitrogen lone pair to the alcohol proton most likely serves

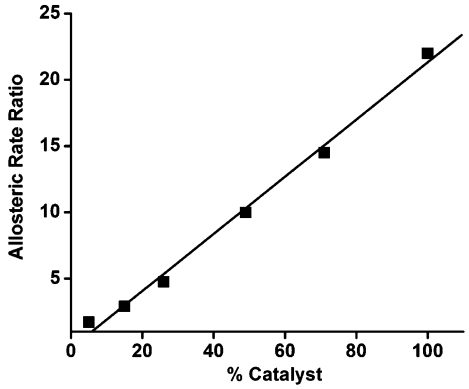

Figure 7. Allosteric rate ratio (R) versus % catalyst (with respect to 4-pyridylcarbinol). R = ratio of 4-acetoxymethylpyridine produced after 6 h by **7** versus **5**. Reactions were monitored by GC-FID. Conditions: CH_2Cl_2, rt, 4-pyridylcarbinol (1.0 mM), acetic anhydride (1 mM), biphenyl (1.5 mM, internal standard), catalyst, CO (1 atm), and benzyltriethylammonium chloride.

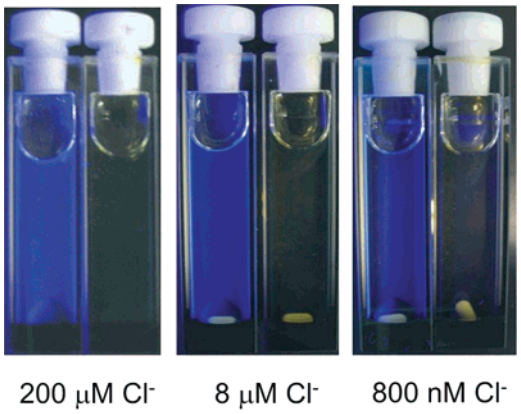

Figure 8. Photograph taken under UV irradiation (365 nm); reaction time = 6 h. Conditions: **5** (0.1 mM), 4-pyridylcarbinol (0.1 mM), acetic anhydride (0.1 mM), diethylaminomethylanthracene (1 mM), CH_2Cl_2, rt, CO (1 atm), benzyltriethylammonium chloride (in given concentration in left vial; no Cl^- in right vial).

to activate the O−H bond for cleavage.[80] Given these observations for 2-pyridylcarbinol, the differences in the reaction rates between **2**, **5**, and **7** can be explained by the accessibility of the Zn^{II} sites for activation of acetic anhydride. The monomer **2** would have the least sterically encumbered sites and, consequently, the highest activity in a solely Lewis-acid activated mechanism. The open catalyst **7** would have both axial sites on each Zn^{II} site available while only one axial site is accessible in **5**. From this explanation, the seemingly unintuitive data fit the model of having two highly activated reagents in the same reaction mixture, which explains the much faster rate of *ortho*-isomer versus that of *meta*- and *para*-isomers. Based upon these studies, one will attain the greatest catalytic rates with the *ortho*-isomer, but the largest allosteric effect and therefore amplification, with the *para*-isomer, which operates via the cooperative bimetallic mechanism.

Signal Amplification and Detection of Cl^- with the Rh^I-Based Allosteric Catalysts. From these studies, optimized conditions for a working system based on this allosteric catalyst were developed. In such a system, the result of an analyte-induced switch to an intramolecular reaction mechanism is a significant increase in the rate of formation of the acylated product, 4-acetoxymethylpyridine, and acetic acid. As a preliminary example of the utility of this novel detection strategy, the detection of Cl^- ions was investigated.[56] Solutions containing fixed mM concentrations of 4-pyridylcarbinol, acetic anhydride, and catalyst were treated with CO over a range of Cl^- ion concentrations. The reactions were initially monitored by GC for the formation of 4-acetoxymethylpyridine. Interestingly, the magnitude of the allosteric effect, which determines the signal-to-noise ratio in our detection scheme, is maximized at high loadings of **5** compared to the catalytic substrates (Figure 7). These product yield enhancements for different catalyst concentrations of open versus closed catalyst are expressed in terms of an allosteric rate ratio. After 6 h, enhancements of approximately 25-fold with respect to product yield are achievable upon activation of **5** with Cl^- under these conditions. In turn, this system responds to a range of Cl^- ion concentrations determined by the concentration of catalyst used, with the greatest amplification measurable as 4-acetoxymethylpyridine formed per mole of Cl^-, occurring for the lowest Cl^- to catalyst ratios. Coupling of this catalytic amplification step to an acid-sensitive fluorophore (diethylaminomethylanthracene) allows for visual and spectrophotometric monitoring of the signal that corresponds to the presence of the analyte.[56] Using this method, concentrations of Cl^- as low as 800 nM were easily observed upon exposure of reaction mixtures to a handheld UV lamp (Figure 8).

Signal Amplification and Detection of Diimines and Isocyanides with the Cu^I-Based Allosteric Catalysts. Utilizing the WLA for the synthesis of these catalysts provides a high degree of tailorability. The inherent modularity of the approach has allowed for detection of different analytes by substituting the structural metal centers of the supramolecular assemblies (Scheme 2). Cu^I-containing macrocycles generated via the WLA have been shown to react with diimine ligands and isocyanides.[67] Thus, a catalytic detection system for these types of molecules based on a Cu^I analogue of **5** was developed (Scheme 3). Before one can begin to probe the ability for these complexes to act as allosteric catalysts, control reactions were required to assess the stability of these complexes under the given reaction conditions. The stabilities of **6** and **8** were measured in solution by $^{31}P\{^1H\}$ NMR spectroscopy when in the presence of all substrates and reagents. The data obtained from these experiments illustrate that compound **6** does not react with any of the reagents (pyridylcarbinol, acetic anhydride, and biphenyl) under catalytic reaction conditions. In the presence of a large excess of pyridylcarbinol (>100 fold), complex **6** reacts to form an open complex similar to **8** in which each Cu^I center is bound to two pyridylcarbinol molecules and two phosphines.[67]

Once the stability of complex **6** was measured, 1,10-phenanthroline (phen) was the first analyte tested using assembly **6**. As seen in Figure 9, a rate enhancement of approximately 7-fold is observed when phenanthroline is added to a reaction mixture containing 4-pyridylcarbinol (1 mM), acetic anhydride (1 mM), and **6** (0.5 mM). Overall, the Rh^I and Cu^I systems exhibit similar catalytic behavior (Figure 10). The magnitude of the allosteric effect in the Cu^I-based system is maximized (approximately 12-fold) at high loadings of **6** with respect to the substrates (Figure 11). The limit of detection for phenanthroline with complex **6** under these conditions was determined to be 200 μM by GC analysis (Figure 12).

(80) Waddell, T. G.; Rambalakos, T.; Christie, K. R. *J. Org. Chem.* **1990**, *55*, 4765−4767.

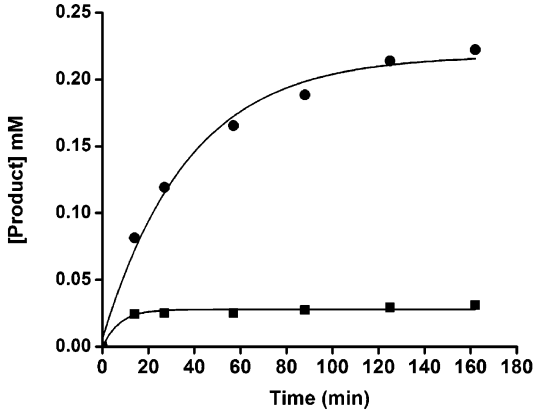

Figure 9. Allosteric control of an acyl transfer reaction using phenanthroline. Conditions: acetic anhydride (1.0 mM), 4-pyridylcarbinol (1.0 mM), biphenyl (1.5 mM, internal standard), catalyst (0.5 mM), CH_2Cl_2, room temperature. ■, **6**; ●, **8**.

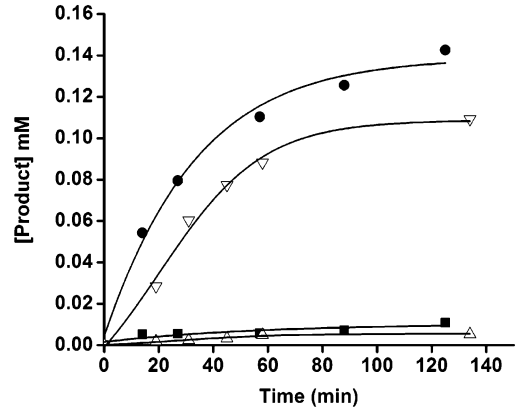

Figure 10. Comparison of Rh^I and Cu^I hinges. Conditions: acetic anhydride (1.0 mM), 4-pyridylcarbinol (1.0 mM), biphenyl (1.5 mM, internal standard), catalyst (0.5 mM), CH_2Cl_2, room temperature. △, **5**; ■, **6**; ▽, **7**; ●, **8**.

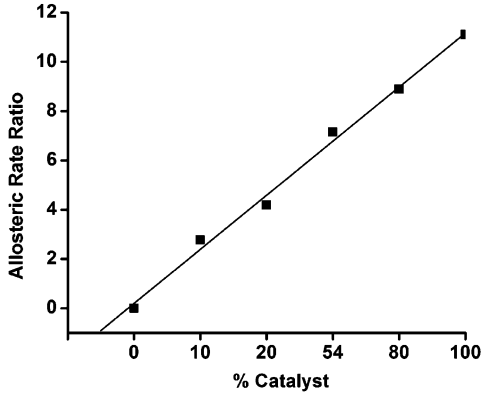

Figure 11. Allosteric rate ratio (R) vs % Catalyst (with respect to pyridylcarbinol). R = the ratio of 4-acetoxymethylpyridine produced after 2.5 hours by **8** vs **6**. Reactions were monitored by GC. Conditions: CH_2Cl_2, rt, 4-pyridylcarbinol (1.0 mM), acetic anhydride (1.0 mM), biphenyl (1.5 mM, internal standard), catalyst.

Unlike Rh^I complex **5**, multiple small molecules can be used to open Cu^I-containing **6**. In addition to phenanthroline, other diimine ligands, such as 2,2′-bipyridine (bipy) and neocuproine, can be used to turn on the intramolecular catalytic cycle, thus increasing the rate of acyl transfer. However, these small molecules provide for less of an allosteric effect than phenanthroline (Figure 13). This effect is due to the ligating properties of the ancillary ligands and their ability to displace the thioether

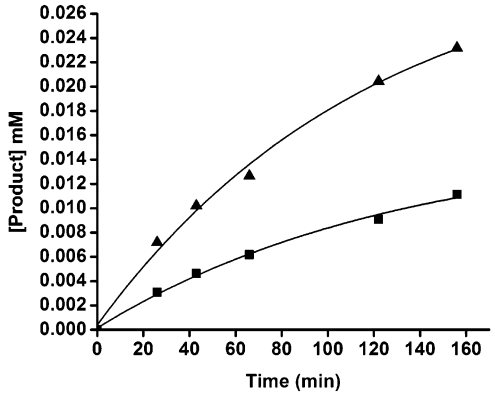

Figure 12. The lower limit of detection for phenanthroline. Conditions: acetic anhydride (0.1 mM), 4-pyridylcarbinol (0.1 mM), biphenyl (0.15 mM, internal standard), catalyst **6** (0.1 mM), 1,10-phenanthroline, CH_2Cl_2, room temperature. ■, **6**; ▲, **6** + 225 μM phen.

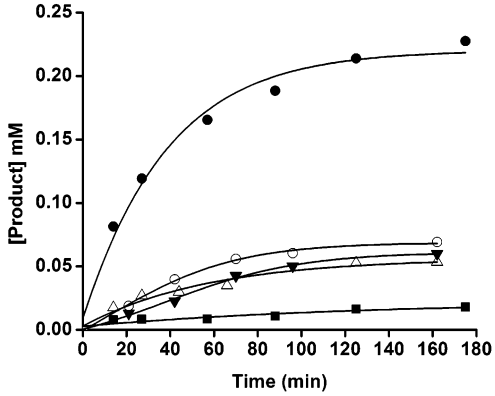

Figure 13. Multiple analyte detection with the CuZn catalysts. Conditions: acetic anhydride (1.0 mM), 4-pyridylcarbinol (1.0 mM), biphenyl (1.5 mM, internal standard), catalyst **6** (0.5 mM), allosteric activator (phen, bipy, neoc, 1.0 mM, or ^{t}BuNC 2.0 mM) CH_2Cl_2, room temperature. ■, **6**; ○, **6** + neoc; ▼, **6** + bipy; △, **6** + ^{t}*B*uNC; ●, **6** + phen.

moieties from the Cu^I sites. In addition to diimines, isonitriles (e.g., ^{t}BuNC) have been detected using the system described above (Figure 13). Again, the allosteric effect brought about by ^{t}BuNC is not as large as when phenanthroline is used. This is likely due to the fact that ^{t}BuNC is a monodentate ligand while phenanthroline is bidentate and, thus, a stronger binder (therefore leading to a greater yield of open catalyst).

Conclusions

The ability to switch between various molecular conformations in situ through the introduction of small molecules has enabled the exploration of a novel detection strategy for these molecules. A critical feature of this detection strategy is that it involves signal amplification through small molecule activation. Hence, the catalytic reaction is a central feature of the strategy, and an understanding of the nature of the allosteric control over various reactions and the arrangement of substrate molecules is of importance to realize the scope of this strategy. These elements include the metal used as a regulatory site and the ancillary ligands, which act as the allosteric effectors capable of binding to the regulatory site, thereby initiating the shape change. By modulating which metal resides in the structure control domain of the allosteric catalyst, the small molecule reactivity of the assembly is altered, which provides a convenient approach for the detection of different analytes. We also have

shown that the activity of the catalyst and, therefore, the allosteric amplification factor is highly dependent upon the binding properties of the regulator. The inherent tailorability of these complexes, which have been prepared via the WLA, bodes well for making designer complexes that have optimized analyte recognition properties coupled to an optimized catalytic amplification event. Our future work will focus on optimization of the catalytic reaction to take into account two distinct factors: (a) turnover frequency of the catalyst and (b) rate differentials between the two states. These are significant challenges that must be overcome to design new supramolecular sensors that exhibit low background reactions and large amplification factors in a reasonable time window.

Acknowledgment. C.A.M. acknowledges the NSF, ARO, and DDRE for support of this research and is grateful to the NIH for a Director's Pioneer Award.

Supporting Information Available: Detailed X-ray structural data including a summary of crystallographic parameters, atomic coordinates, bond distances and angles, anisotropic thermal parameters, and H atom coordinates for **3**, in CIF format. This material is available free of charge via the Internet at http://pubs.acs.org.

JA0711516